Quaternary Science Reviews 30 (2011) 2976–2987

Contents lists available at ScienceDirect

Quaternary Science Reviews

journal homepage: www.elsevier.com/locate/quascirev

Suborbital-scale surface and deep water records in the subtropical North Atlantic: implications on thermohaline overturn

Katharina Billups [a,*], Nathan Rabideaux [b], Jared Stoffel [c]

[a] University of Delaware, 700 Pilottown Road, Lewes, DE 19958, USA
[b] Rensselaer Polytechnic Institute, 110 8th St. Troy, NY 12180, USA
[c] University of Dayton, 300 College Park, Dayton, OH 45409, USA

ARTICLE INFO

Article history:
Received 28 February 2011
Received in revised form
16 June 2011
Accepted 22 June 2011
Available online 15 August 2011

Keywords:
Paleoceanography
Millennial-scale
Stable isotopes
Foraminifera

ABSTRACT

We reconstruct millennial-scale variations in sea surface hydrography and deep water flow in the northwestern subtropical Atlantic (Ocean Drilling Program Leg 172 Sites 1056 and 1063) with a focus on Marine Isotope Stage (MIS) 9. Together with published records from this region, the new data also afford a longer-term perspective on millennial-scale changes in meridional overturning circulation spanning two full interglacial intervals (MIS 9 and 11) as well as two full glacial intervals (MIS 10 and 12). Planktic foraminiferal $\delta^{18}O$ values indicate relatively stable conditions during the peak warmth of MIS 9, but three large cold excursions disrupt the otherwise smooth transition toward glacial MIS 8. There is no unique response in the Site 1063 benthic foraminiferal $\delta^{13}C$ values that would suggest a concomitant decrease in the relative flux of NADW during these events. Similarly, there is no persistent correlation between millennial-scale variations in surface and deep water hydrography over the entire MIS 8–13 interval. While millennial-scale variations at the sea surface are most pronounced during glacial intervals (and the transitions toward glacial intervals), millennial-scale variations in the deep water hydrography tend to be largest during the warm periods. This observation supports that rapid changes in thermohaline circulation are sensitive to driving forces other than those directly related to ice sheet size. Time series analysis shows that spectral power in the benthic foraminiferal $\delta^{13}C$ record contains periodicities related to the second (~10 kyr) and fourth harmonics (~5 kyr) of precession in this record (~20 kyr) pointing to the importance of tropical processes.

1. Introduction

Two main mechanisms have been proposed to explain millennial-scale changes in thermohaline overturn. During intervals of glaciations high latitude ice sheets, and in particular their meltwater, affect millennial-scale fluctuations in deep water circulation (e.g., MacAyeal, 1993; Oppo and Lehman, 1995; Mayewski et al., 1997; Schulz et al., 1999; Benway et al., 2010). Broecker et al. (1990) were the first to propose a model relating millennial-scale climate fluctuations observed in Greenland ice core records to thermohaline circulation. McManus et al. (1999), however, observe that in the subpolar North Atlantic, millennial-scale deep water proxy variations persist through interglacial intervals suggesting that other processes are important controls on deep water formation on this scale. Low latitude surface water hydrographic variations may be important controls on meridional overturning via poleward heat transport in surface current and subsequent deep water formation (Boyle and Keigwin, 1987; Vidal et al., 1997; Chapman and Shackleton, 1998; Rühlemann et al., 1999; Hagen and Keigwin, 2002; Healey and Thunell, 2004; Schmidt et al., 2006; Benway et al., 2010). A recent study finds correlation between high frequency surface and deep water variations in the North Atlantic and tropical insolation forcing illustrating the importance of tropical forcing on meridional overturning circulation during mid Pleistocene glacial and interglacial stages (Ferretti et al., 2010).

Millennial-scale climate variability during Pleistocene interglacial intervals has been studied extensively because of the potential to provide analogs for Holocene climate stability. Among these, Marine Isotope Stage (MIS) 11 has received much attention because insolation forcing, in particular low eccentricity values, is similar to insolation forcing of the Holocene (Bauch et al., 2000; Hodell et al., 2000; Droxler et al., 2003; Dickson et al., 2009). Numerous studies have illustrated that MIS 11 climate was relatively stable at high latitudes (Oppo et al., 1998; McManus et al., 1999, 2004). However, relatively large instabilities, or cold events, characterize this

* Corresponding author. Tel.: +1 302 645 4249.
E-mail address: kbillups@udel.edu (K. Billups).

0277-3791/$ – see front matter © 2011 Elsevier Ltd. All rights reserved.
doi:10.1016/j.quascirev.2011.06.015

interval of warmth in the subtropical Atlantic where these events can be related to changes in deep water circulation (Billups et al., 2004).

MIS 9 has received far less targeted attention from the paleoceanographic community although some argue that it is a better analog for Holocene insolation forcing than MIS 11 (Ruddiman, 2007). The analogy arises because the amplitude of the insolation minimum is similar between these two interglacial periods due to the relative phasing of obliquity and precession (Ruddiman, 2007). There are millennial-scale records that span MIS 9 in the Atlantic Ocean (e.g., McManus et al., 1999; Helmke and Bauch, 2003; Voelker et al., 2010; in press), but few studies have concentrated on MIS 9 climate *per se*. High resolution studies of MIS 9 have focused on depositional changes in the subtropical Atlantic (Franz and Tiedemann, 2002) and vegetation changes in southwestern Europe (Desprat et al., 2008). Thus far, no studies have addressed millennial-scale changes in subtropical Atlantic surface water hydrography or deep water circulation during MIS 9.

We reconstruct millennial-scale changes in meridional overturning circulation in the northwestern subtropical Atlantic with a specific focus on interglacial/glacial events of MIS 9 and 8 (334–260 Ka) and then take a broader view on late Pleistocene glacial and interglacial stages (MIS 13–8; 500–260 Ka). A depth transect of sites was drilled during Ocean Drilling Program (ODP) Leg 172 in the sediment drift along the Blake Bahama Outer Ridge (BBOR) and the Bahama Bank (Fig. 1) designed to reconstruct suborbital climate variability in the northwestern subtropical Atlantic (Keigwin et al., 1998). We generate new planktic and benthic stable isotope data for two of these sites, Site 1056 and 1063, in order to reconstruct variations in surface and deep water hydrography, respectively. We hypothesize that a correlation between surface and deep water records in the subtropical Atlantic on the millennial-scale supports a link between poleward heat transport in the surface ocean and high latitude deep water formation (e.g., Oppo et al., 2001; Keigwin and Jones, 1994). Planktic and benthic foraminiferal stable isotope records at these sites have been published for MIS 10–13, and we put together a composite that encompasses two full interglacial (MIS 11 and MIS 9) and two full glacial intervals (MIS 12 and 10). The length of this record (250 kyr) allows statistical tests for the presence or absence of significant concentration of power at millennial-scale periodicities through time.

Table 1
Summary of site locations and references for data sources.

Site	Long/Lat (°)	Water Depth	MIS[a]	Type[b]	Reference
1056	76W/32N	2167 m	8–10.2	PF	This study
			10–12	PF	Billups et al. (2004)
			8–10.2	BF	Franz and Tiedemann (2002)
			10–13	BF	Chaisson et al. (2002)
1063	58W/34N	4583 m	8–10.2	BF	This study
			10–13	BF	Poli et al. (2000)
1058	75W/32N	2984 m	12–13	PF	Billups et al. (2006)
980	15W/55N	2179 m	8–13	BF	McManus et al. (1999)
U1308	24W/50N	3872 n	8–13	BF	Hodell et al. (2008)

[a] MIS stands for Marine Isotope Stage.
[b] Type refers to benthic foraminifera (BF) or planktic foraminifera (PF).

2. Approach

2.1. Hydrographic setting

The northwestern subtropical Atlantic is an ideal region to study the relative stability of surface and deep ocean hydrography because its role in meridional overturning circulation. ODP Site 1056, the focus of our surface hydrographic reconstructions, was drilled on BBOR at about 32°N, 76°W (~2200 m water depth, Table 1), underlying the warm waters of the northwestern limb of the subtropical gyre, close to the northern boundary of the Gulf Stream (e.g., Fig. 1). The Gulf Stream is a major component of the North Atlantic climate system and thermohaline overturn (Schmitz and McCartney, 1993). It transports warm surface water to high northern latitudes and contributes to North Atlantic warm anomalies of up to ~10 °C (Rahmstorf, 2002). Winter time cooling of the relatively warm surface, as well as seasonal sea ice and associated brine formation, contribute to deep convection and deep water mass formation in the subpolar gyres of the North Atlantic (North Atlantic Deep water, NADW e.g., Pickard and Emery, 1990). The deep water masses then flow southward. In the deep equatorial Atlantic, NADW and Antarctic Bottom Waters (AABW) meet and mix in proportions relative to the strength of their formation at the source areas. Site 1063 (34°N, 58°W, ~4600 m water depth, Table 1), the focus of the deep water mass reconstructions, lies close to the modern day mixing zone of NADW with AABW

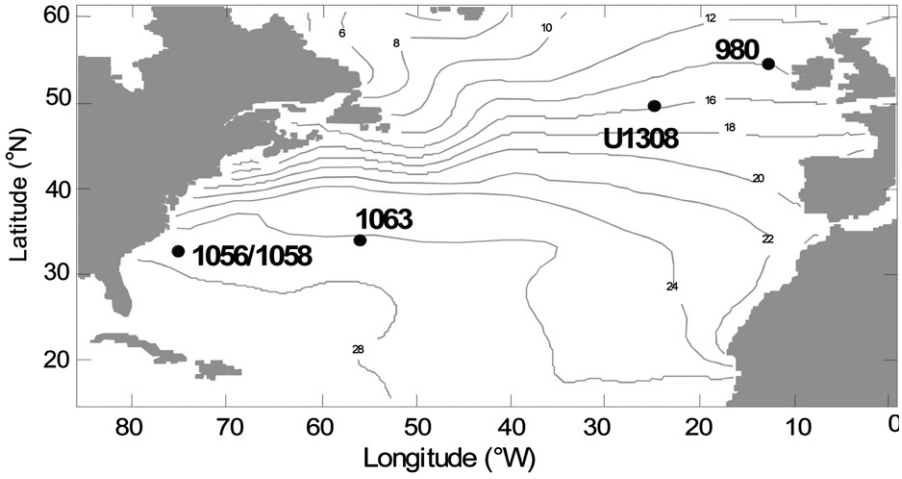

Fig. 1. Location of Sites 1056 (32°N, 76°W, 2167 m) and 1063 (34°N, 58°W, 4583 m) with respect to average late summer sea surface temperatures (Levitus and Boyer, 1994). Also shown are the location of Sites 980 (55°N, 14°W, 2179 m) and U1308 (50°N, 24°W, 3872 m), which are important monitors of the $\delta^{13}C$ of dissolved inorganic carbon in deep water. The figure was generated using the interactive web site of the Lamont Doherty Geological Observatory.

(Keigwin et al., 1998) and is thus well placed to monitor changes in the relative flux of these water masses through time.

2.2. Reconstructing surface water hydrography

Planktonic foraminiferal stable isotope records are commonly used proxies for reconstructions of surface water hydrography. The $\delta^{18}O$ variations of planktic foraminifera reflect the $\delta^{18}O$ of seawater and the water temperature at the time of calcification. The $\delta^{18}O$ of seawater varies primarily as a function of ice volume, the amplitude of which is probably relatively small on the millennial-scale. Thus the signal is likely dominated by changes in the surface water temperature and evaporation versus precipitation (salinity) patterns. The effect of changes in the $\delta^{18}O$ of seawater due to salinity variations is expected to be small because the slope of the $\delta^{18}O$/salinity relationship in the region (Sargasso Sea/Gulf Stream waters) is shallow, 0.11 per mil/psu (Fairbanks et al., 1992), and the modern seasonal salinity range in this region is only 0.3 (Levitus et al., 1994). Thus, unless large changes occurred in the meridional position of the Gulf Stream, which are unlikely (Matsumoto and Lynch-Stieglitz, 2003), the millennial-scale variations in the foraminiferal $\delta^{18}O$ values are likely dominated by sea surface temperature variability in the western boundary current. This does not rule out, however, that changes in surface water salinity linked to variable sea surface temperatures within the Gulf Stream may not have affected the planktic foraminiferal $\delta^{18}O$ values.

We construct the surface hydrography using the $\delta^{18}O$ values of *Globigerinoides ruber* (white). In the subtropical setting of Site 1056, *G. ruber* occupy the upper mixed layer of the water column and calcify throughout the year, but test production is highest during the warmer summer months (Deuser, 1987). *G. ruber* (white) occur as two morphotypes referred to as senso stricto (s.s.) and senso lato (s.l.), which differ in the shape of the last chamber and their isotopic composition (Wang, 2000; Löwenmark et al., 2005). At nearby Site 1058, Billups et al. (2006) measured the stable isotopic composition of both morphologies in 38 intervals and found an offset similar to the published one correcting *G. ruber* (s.s.) values to those of *G. ruber* (s.l.), which dominate that record. The Site 1056 samples from MIS 9 are entirely based on *G. ruber* s.l., and no correction is necessary.

The new results from MIS 9 extend toward the present previously published planktic foraminiferal stable isotope reconstructions of the sea surface hydrography in this region (Table 1). We join the *G. ruber* $\delta^{18}O$ record from MIS 9 with the MIS 10/11 *Globigerinoides sacculifer* $\delta^{18}O$ record from Site 1056 (Billups et al., 2004) and append the *G. ruber* $\delta^{18}O$ from nearby Site 1058 (Fig. 1) to include MIS 12 and portions of MIS 13 (Billups et al., 2006). Billups et al. (2006) illustrate that the millennial-scale variations recorded by *G. ruber* and *G. sacculifer* are similar, with *G. ruber* recording slightly higher amplitude variations than *G. sacculifer*. Together the composite record spans 250 kyr and allows us to statistically test for the significance of climate instabilities during two full interglacial (MIS 9 and 11) and two full glacial (MIS 10 and 12) intervals.

2.3. Reconstructing deep water circulation

We reconstruct deep water circulation in the northwestern Atlantic using the $\delta^{13}C$ values of benthic foraminifera from Site 1063 (Fig. 1, Table 1). Thunell et al. (2002) illustrate that among the sites drilled in the subtropical Atlantic during Leg 172, Site 1063 is the most sensitive to variations in the relative flux of deep waters during interglacial MIS 11, and presumably during MIS 9.

In the modern ocean, NADW is characterized by relatively high $\delta^{13}C$ values of total dissolved inorganic carbon (ΣCO_2) ($\sim$ 1 per mil) reflecting the influence of nutrient poor source waters originating in the subtropical northwestern Atlantic while AABW, derived from more nutrient enriched circum Antarctic Southern Ocean, has lower $\delta^{13}C$ values ($\sim$0.3 per mil) (e.g., Curry et al., 1988). In the modern ocean, at Site 1063 the $\delta^{13}C$ values are relatively high ($\sim$0.9 per mil) due to the high proportion of northern-sourced waters at $\sim$4600 m water depth (Fig. 2).

Benthic foraminiferal $\delta^{13}C$ records are commonly used to reconstruct vertical profiles of the $\delta^{13}C$ of ΣCO_2 to infer changes in the relative flux of northern versus southern sourced deep waters and hence thermohaline circulation in the Atlantic Ocean (see Mackensen and Bickert, 1999 for a review). The approach necessitates a number of assumptions including adequate characterization of source water $\delta^{13}C$ values, which can change as a function of biological (nutrient utilization) and physical (air-sea gas exchange) processes. To characterize source water $\delta^{13}C$ variability during MIS 9/8 we use the published benthic foraminiferal $\delta^{13}C$ data from Site 1056 (Franz and Tiedemann, 2002). This relatively shallow site ($\sim$2200 m water depth) remains close to the core of northern-sourced waters even during glacial intervals (Franz and Tiedemann, 2002; Thunell et al., 2002). Using this site is ideal as the planktic foraminiferal data are generated from samples immediately adjacent to the core intervals sampled by Franz and Tiedemann (2002) eliminating age control uncertainties. To interpret the composite record spanning MIS 8–13 with respect to changes in deep water hydrography, we use North Atlantic Site 980 (McManus et al., 1999) as well as U1308 (Hodell et al., 2008) as monitors of northern source water $\delta^{13}C$ values. Site 980 at 2179 m water depth lies within the flow of upper NADW while U1308, at 3872 m water depth, is bathed by lower NADW. Changes in the gradient between $\delta^{13}C$

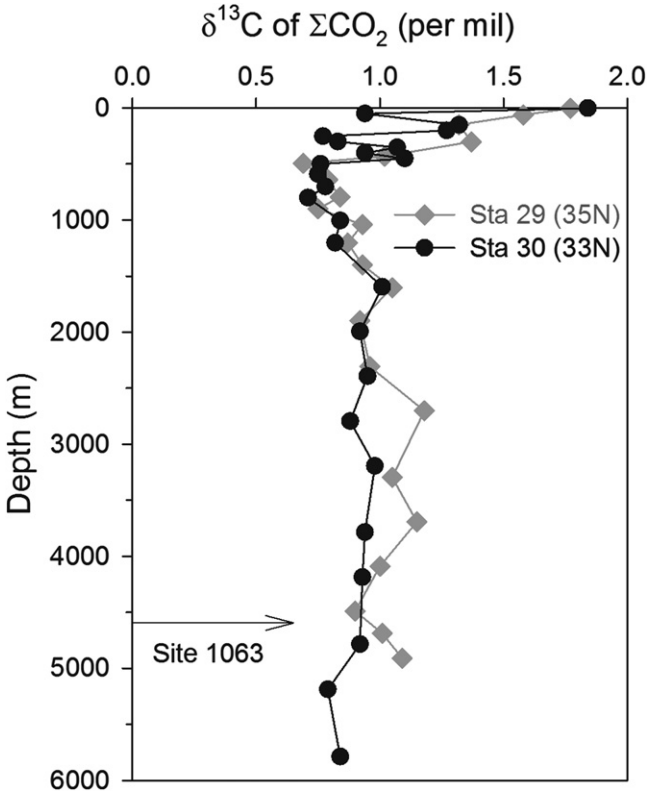

Fig. 2. Vertical water column $\delta^{13}C$ profiles at GEOSECS stations 29 and 30 (Kroopnick, 1985), which bracket the location of Site 1063 (34°N) in the northwestern subtropical Atlantic. At the water depth of Site 1063 ($\sim$4600 m), $\delta^{13}C$ values of dissolved inorganic carbon (ΣCO_2) are relatively high ($\sim$0.9 per mil) reflecting the relatively large proportion of North Atlantic Deep Water at this depth in the modern ocean.

values at Site 1063 and Site 980 have been interpreted as variations in the relative flux of NADW versus AABW, a reflection of the strength of meridional overturning circulation (e.g., Dickson et al., 2009). Deeper Site U1308 provides an additional constraint on water mass geometry closer to the water depth of Site 1063. We highlight that deep water circulation studies using benthic foraminiferal $\delta^{13}C$ records consider the relative flux of water masses rather than production rates, which are beyond the limits of this tracer.

Usually, *Cibicidoides* are used for deep water reconstructions because their $\delta^{13}C$ values reflect the $\delta^{13}C$ of ΣCO_2 (see for example, Mackensen and Bickert, 1999). At sediment drift Site 1063, a continuous record could only be constructed by combining *Oridorsalis umbonatus* measurements with *Cibicidoides mundulus* data. In order to constrain species effects on the stable isotopic composition of the tests, we have measured both species at all possible intervals (n = 20) (Fig. 3). Duplicate measurements on these 20 intervals reveal an average $\delta^{18}O$ offset of -0.59 ± 0.16 per mil and a $\delta^{13}C$ offset of 1.19 ± 0.36 per mil; the *O. umbonatus* data are corrected accordingly. Although this species is not commonly used as a tracer for deep water circulation it has been included in such studies (e.g., Billups et al., 2002). Furthermore, other published deep water records from this region contain measurements from this species as well (Franz and Tiedemann, 2002). As shown in Fig. 3, the $\delta^{13}C$ values of *O. umbonatus*, when continuously present at high resolution (at 69–71 mcd), trace millennial-scale signals outlined by the *C. mundulus* (Fig. 3, top panel).

The new results from MIS 9 extend toward the present previously published benthic foraminiferal stable isotopic records from this site (Table 1). We join the $\delta^{18}O$ record from MIS 8/9 with the MIS 10/13 $\delta^{18}O$ record from Poli et al. (2000). Together the composite record spans 250 kyr and allows us to statistically test for the significance of instabilities in thermohaline overturn during two full interglacial (MIS 9 and 11) and two full glacial (MIS 10 and 12) intervals.

3. Methods

3.1. Sampling and analytical methods

We have sampled the MIS 9 section of the sediment cores from Sites 1056 and 1063 at 5 cm intervals. This sampling rate results in an average temporal resolution of ~500 years at Site 1056, which is sufficient to resolve millennial-scale variations to periodicities of ~3–4 kyr (e.g., 6–8 data points per cycle). At Site 1063, the sampling interval yields a ~300 yr time step. However the record contains gaps due to the lack of either *Cibicidoidies* or *Oridorsalis*, and the effective time step is closer to 500 years, on average.

Sediments were processed following standard procedures, which include oven drying overnight, dissociation in a buffered sodium hexametaphosphate solution, and wet sieving (63 μm). About 10–15 *G. ruber* (white) tests were measured from the 255–350 μm size fraction to minimize size effect on the stable isotope values. About 1–3 tests of *Cibicidoides* spp. and *Oridorsalis* were selected from the >250 μm size fraction. All samples were sonicated in deionized water to remove fine grained particles and then oven dried overnight prior to stable isotopic analyses.

Stable isotope analyses were conducted at the University of Delaware using a GV Instruments IsoPrime dual inlet stable isotope ratio mass spectrometer equipped with a Multiprep sample preparation system for the analysis of individual samples. The analytical precision of the instrument is better than 0.08 per mil for $\delta^{18}O$ and 0.06 per mil for $\delta^{13}C$ in a size range of 20–200 μg. The values are recorded versus VPDB using an in-house standard (Carrara Marble) and NBS-19.

3.2. Age control

Uniform age control was established for all Leg 172 sites (BBOR and Bermuda Rise) by Grützner et al. (2002) by tuning color reflectance records to orbital precession. In their study of MIS 9 and 8, Franz and Tiedemann (2002) have increased the temporal resolution of the Site 1056 age control points by aligning individual features of the $\delta^{18}O$ record to marine isotope substages 8.3–10.2. We use this revision as it allows a direct comparison of our MIS 9 planktic $\delta^{18}O$ data with the benthic foraminiferal stable isotope record of Franz and Tiedemann (2002).

For the purpose of correlating the deep water Site 1063 with the surface water records from Site 1056 during MIS 9, we align the benthic foraminifera stable isotope record from Site 1063 with Site 1056 using $\delta^{18}O$ maxima and minima associated with substages of MIS 9 and 8 (Fig. 4). According to this age model, the timing of the rapid deglaciation following MIS 10 (Termination IV) is at 334 Ka, which is 3 kyr younger than the age of Termination IV on other age models (e.g., 337 Ka, Lisiecki and Raymo, 2005). The discrepancy is likely due to different assumptions underlying the tuning strategies. For the MIS 9 focus, however, the absolute ages are less critical than the correlation between Sites 1056 and 1063. We concede that

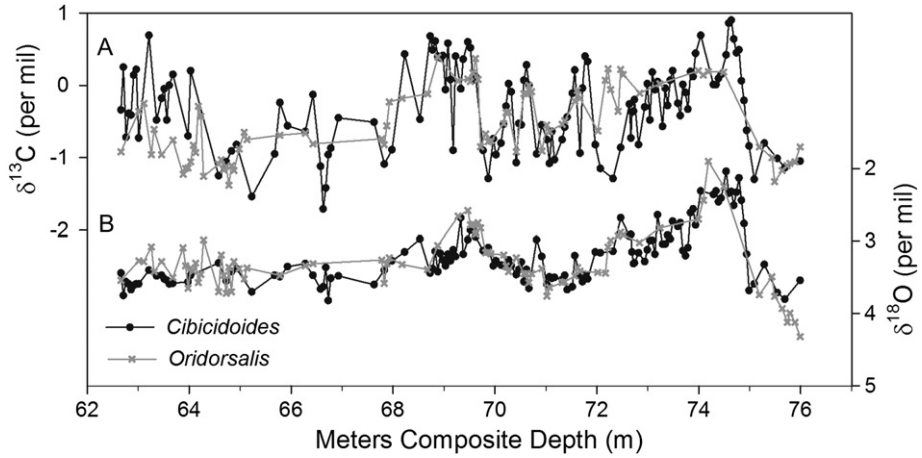

Fig. 3. Comparison of Site 1063 *Cibicidoides mundulus* (black circles) and *Oridorsalis umbonatus* (grey crosses) $\delta^{13}C$ (A) and $\delta^{18}O$ (B) records on the depth scale. The *Oridorsalis* data have been adjusted to *Cibicidoides* to account for species offsets ($\delta^{18}O$: −0.59; $\delta^{13}C$: 1.19 per mil). Both species exhibit millennial-scale variations in the $\delta^{13}C$ values (i. e. at 69–71 mcd) supporting their combined use to obtain a more continuous record.

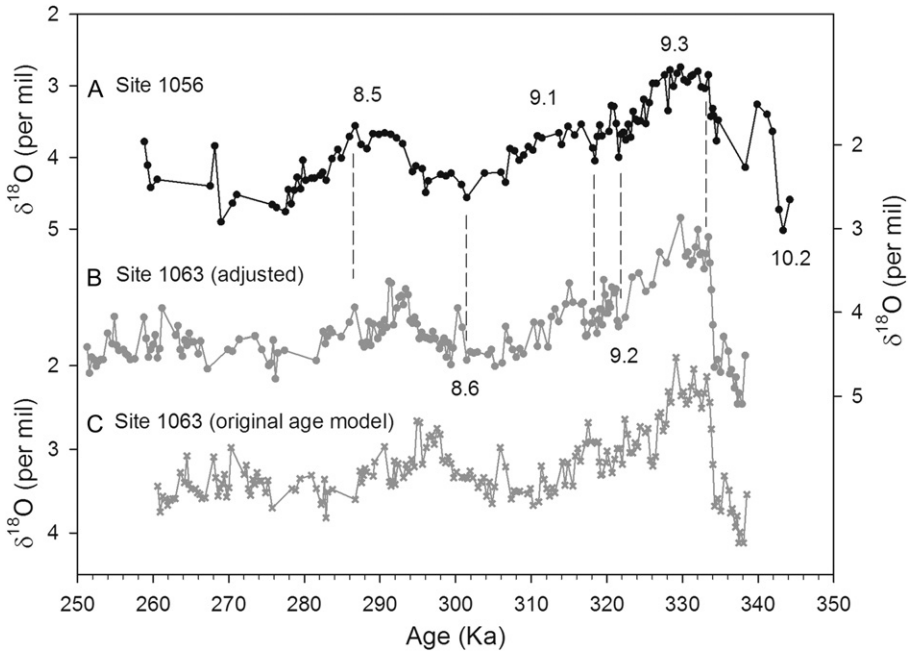

Fig. 4. Correlation of the Site 1063 benthic foraminiferal $\delta^{18}O$ record (grey circles, B) to the Site 1056 benthic foraminiferal $\delta^{18}O$ record (black circles, A, Franz and Tiedemann, 2002). The Site 1063 record on the original age model of Grützner et al. (2002) is also shown (grey crosses, C). The records are correlated using the $\delta^{18}O$ maxima and minima associated with the individual substages of the Marine Isotope Stages 9 and 8 (dashed vertical lines).

uncertainties in the correlation of relatively small features in the $\delta^{18}O$ records may introduce uncertainties in the correlation of the surface (planktic foraminiferal $\delta^{18}O$ from Site 1056) and deep water (benthic foraminiferal $\delta^{13}C$ from Site 1063). This limits detailed comparisons of individual maxima and minima in one record versus the other.

3.3. Time series analysis

We use wavelet analyses (Wavelet software is provided by *C. Torrence and G. Compo*, and is available at URL: http://paos.colorado.edu/research/wavelets/) to test for significance, and to summarize the evolution, of the millennial-scale periodicities in the composite surface (Site 1056/1058 planktic foraminifera) and deep water records (Site 1063 benthic foraminifera). Because the Site 1063 $\delta^{13}C$ record contains a disproportionally large number of gaps after 280 ka, we truncate the records at that point. Using the Arand software package (Howell et al., 2006), the records were first interpolated a constant 500 year intervals, and then high pass filtered to remove orbital-scale variations (>25 kyr) that dominate the records. Assuming a red noise model, we set a 90% confidence interval.

In order to better resolve millennial-scale periodicities in the benthic foraminiferal $\delta^{13}C$ record, spectral analyses are also conducted using standard Blackman-Tukey techniques using the Arand software package (Howell et al., 2006). The truncated and interpolated record (500 year time step) was then detrended and remaining gaps coded as missing values (−9999). The confidence level was set to 80%.

4. Results: MIS 9

4.1. Orbital-scale observations

The MIS 9 through MIS 8 study interval at Site 1056 contains three prominent maxima in Northern Hemisphere summer insolation, the larger two being readily apparent in the *G. ruber* as well as benthic foraminiferal $\delta^{18}O$ minima (at 330 Ka, MIS 9.3 and at 290 Ka, MIS 8.5, Fig. 5A–C). While these $\delta^{18}O$ minima are distinct in all three records, the $\delta^{18}O$ minimum that would correlate to the smaller of the precession maxima (MIS 9.1 at 310 Ka) is not well expressed in the *G. ruber* $\delta^{18}O$ record because of three rather large positive $\delta^{18}O$ excursions that overprint the longer-term trend (Fig. 5B). MIS 9.1 does show up as a minor minimum in both benthic foraminiferal $\delta^{18}O$ records (Fig. 5C). In fact, Fig. 5C illustrates the excellent agreement to which these records can be brought on the orbital as well as suborbital-scale.

The two benthic foraminiferal $\delta^{13}C$ records show distinct differences with generally lower values at the deeper than the shallower site (Fig. 5D). There are intervals of time when $\delta^{13}C$ maxima at the deeper site (~0.6–0.7 per mil) reach $\delta^{13}C$ minima at the shallower site; during the peak of interglacial MIS 9 (MIS 9.3, ~325–335 Ka) and during a warming within glacial MIS 8 (MIS 8.5, 288–292 Ka). Site 1063 $\delta^{13}C$ maxima also approach Site 1056 values at ~295–300 Ka, and at ~307–315 Ka, but the values are lower (0.3–0.4 per mil) and the fluctuations are large with $\delta^{13}C$ minima akin to glacial values (~−1 per mil). Linear regression between the Site 1063 $\delta^{18}O$ and $\delta^{13}C$ values shows that the two variables are inversely correlated ($r = 0.48$, $P < 0.0001$, Fig. 6). $\delta^{13}C$ values of southern component deep water are never higher than ~0.0–0.3 per mil (Hodell et al., 2003), which rules out that increases in the $\delta^{13}C$ of southern sourced deep water (e.g., AABW) during interglacial intervals is responsible for relatively high values at Site 1063. Therefore, these results are consistent with enhanced proportion of ^{13}C enriched northern component deep waters into the deeper Atlantic during interglacial, or rather, as is the case for MIS 8.5, during relatively warm intervals. These orbital-scale $\delta^{13}C$ variations at Site 1063 during MIS 9 and 8 are typical of such fluctuations in the North Atlantic Ocean (e.g., Curry et al., 1988; Raymo et al., 1990; Bickert et al., 1997).

During the deglaciation from MIS 10 to MIS 9 (Termination IV) all records change rather synchronously (Fig. 5). Site 1063 benthic

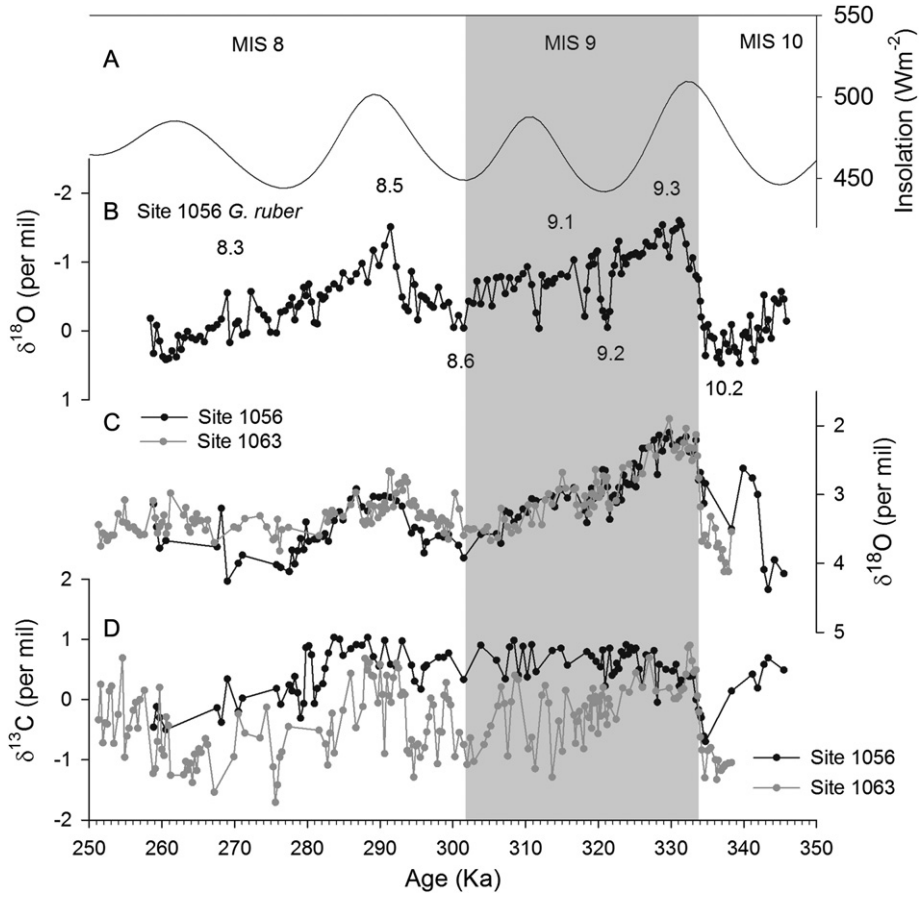

Fig. 5. Results from Marine Isotope Stage (MIS) 9 showing a comparison of Northern Hemisphere summer insolation (Laskar et al., 1993, A) with the Site 1056 *Globigerinoides ruber* $\delta^{18}O$ record (B), the Sites 1056 (black circles, Franz and Tiedemann, 2002) and 1063 (grey circles) benthic foraminiferal $\delta^{18}O$ records (C), and the Sites 1056 (black circles, Franz and Tiedemann, 2002) and 1063 (grey circles) benthic foraminiferal $\delta^{13}C$ records (D). The grey vertical shading highlights interglacial MIS 9 and the numbers refer to substages.

foraminiferal $\delta^{13}C$ values increase rapidly concurrent with the decrease in the corresponding $\delta^{18}O$ values (Fig. 5C and D, respectively). Within the constraints of the age model, the $\delta^{18}O$ decrease at Site 1063 is therefore coincident with the decrease in the planktic foraminiferal $\delta^{18}O$ values at Site 1056 (Fig. 5B). Assuming that the global ice volume decrease across Termination IV is equivalent to a ~1.6 per mil decrease in benthic foraminiferal $\delta^{18}O$ values (Lisiecki and Raymo, 2005), and that the planktic foraminiferal $\delta^{18}O$ decrease reflects synchronous changes in ice volume and SSTs, the magnitude of the decrease in the planktic foraminiferal $\delta^{18}O$ of ~1.8–2 per mil leaves room for a 1–2 °C sea surface warming (via the paleotemperature equation of Erez and Luz, 1982). Similarly, during the transition from the glacial maximum of MIS 8 to the relatively warmer substage MIS 8.5, Site 1063 $\delta^{13}C$ values increase abruptly at 293 Ka as planktic $\delta^{18}O$ values decrease between 294 Ka and 292 Ka (Fig. 5B and D). The close temporal succession of deep and surface water changes seen in these records is similar to the relationship observed between mid-depth $\delta^{13}C$ records and sea surface temperatures in the North Atlantic (Lisiecki and Raymo, 2009). The timing observed here with respect to the deep ocean implies a close relationship between climatic warming and meridional overturning circulation during these particular deglaciations.

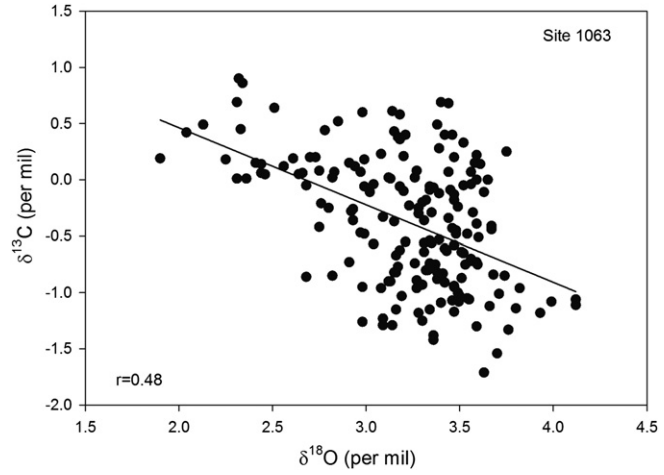

Fig. 6. Scatter plot of Site 1063 $\delta^{18}O$ versus $\delta^{13}C$ values. The two variables are significantly correlated ($r = 0.48$, $P < 0.0001$) reflecting the dominance of a ^{13}C enriched deep water mass during interglacial intervals and a ^{13}C depleted water mass during glacial intervals as expected from deep water circulation changes.

4.2. Millennial-scale signals

On the suborbital-scale, the most prominent feature of the *G. ruber* record is a series of unusually large positive excursions that punctuate the otherwise smoothly increasing values from the MIS 9 minimum toward glacial MIS 8 (Fig. 5B). These excursions are outlined by two or more data points and are thus not aberrant

values but real climatic events, the oldest of which corresponding to MIS 9.2 (~321 Ka). Planktic foraminiferal $\delta^{18}O$ values increase by ~0.8–1 per mil at 321 Ka, 318 Ka, and at 312 Ka (Fig. 5B). These $\delta^{18}O$ maxima approach values more typical of full glacial conditions (e.g., ~0 per mil) but do not have equivalently large features in the benthic foraminiferal $\delta^{18}O$ record from this site (Fig. 5C). The youngest event (312 Ka), is not apparent at all in the benthic foraminiferal record. The magnitude of the $\delta^{18}O$ signal is at least twice the degree of increase in the same site benthic foraminiferal $\delta^{18}O$ values suggesting that the $\delta^{18}O$ maxima are distinct sea surface cooling events (on the order of ~2 °C). There is no unique response in the Site 1063 benthic foraminiferal $\delta^{13}C$ values, however, that would suggest a concomitant decrease in the relative flux of NADW during these events (Fig. 5D).

In fact, throughout the record fluctuations in benthic $\delta^{13}C$ values do not seem to be associated with variation in planktic $\delta^{18}O$ values. Pronounced $\delta^{13}C$ oscillations (>1 per mil) occur between 306 and 315 Ka and at ~296–300 Ka, both times lacking correspondingly large $\delta^{18}O$ variations (Fig. 5D and B, respectively). Relatively well defined, higher amplitude $\delta^{13}C$ fluctuations (~ 0.5 per mil) also characterize the two warm intervals MIS 9.3 and MIS 8.5. While MIS 9.3 also contains suborbital-scale peaks in the planktic $\delta^{18}O$ record, which might support a surface and deep water link at this time, during MIS 8.5, the benthic $\delta^{13}C$ values are not related to any obvious features in the planktic $\delta^{18}O$ record.

5. Beyond MIS 9: a longer-term view

5.1. Age control

The Site 1056 and Site 1063 stable isotope records constructed here extend the published records of Billups et al. (2004, 2006) and Poli et al. (2000) allowing a comparison of the instabilities in surface and deep water hydrography spanning two full interglacial (MIS 9 and MIS 11) and two full glacial intervals (MIS 12 and MIS 10). Spliced together we obtain a 250 kyr long record of surface and deep water variability spanning the late stages of MIS 13 through MIS 8 (500–250 Ka) (Table 1).

To report all records on a common time scale, we align benthic foraminiferal $\delta^{18}O$ records from Site 980 (McManus et al., 1999), Site U1308 (Hodell et al., 2008), Site 1063 (Poli et al., 2000 and this study), and Site 1056 (Franz and Tiedemann, 2002; Chaisson et al., 2002) with the global stack of Lisiecki and Raymo (2005) (thereafter referred to as LR04, Fig. 7). We include the Site 980 and U1308 $\delta^{13}C$ records as northern source deep water endmembers because the $\delta^{13}C$ record from Site 1056 is not published beyond MIS 9. But we can use the, albeit low resolution, Site 1056 $\delta^{18}O$ record to transfer the LR04 time scale to the planktic record from this site. This leaves a ~40 kyr portion of the planktic foraminiferal $\delta^{18}O$ record between MIS 12 and MIS 13 (from Site 1058, Billups et al., 2006) for which we do not have corresponding benthic foraminiferal $\delta^{18}O$ data. We use the *G. ruber* $\delta^{18}O$ record directly to align the timing of MIS 12/13 with LR04. We use $\delta^{18}O$ maxima and minima corresponding to the major isotope stages as well as substages as control points (Fig. 7). In addition, because of the identical shape of the MIS 12/MIS 11 deglaciation in all records, we use the age of Termination V, 424 Ka (Lisiecki and Raymo, 2005), to further synchronize the records. We then linearly interpolate between the control points to derive ages for all data points. Synchronization of $\delta^{18}O$ records using the age of terminations has been called into question because of a different response time of deep water temperatures in the Pacific versus Atlantic Ocean (Skinner and Shackleton, 2005; Lisiecki and Raymo, 2009). As we are only comparing sites within the North Atlantic basin, this uncertainty is probably minor.

5.2. Relative stability of surface and deep water hydrography

Aligning the orbital-scale $\delta^{18}O$ maxima and minima also brings into agreement individual smaller, presumably millennial-scale, features in the $\delta^{18}O$ records. During MIS 12 (at 440 Ka), there is a relatively large $\delta^{18}O$ decrease just prior to the glacial maximum. The warming event is most pronounced in the subtropical sea surface where it is reflected in a ~2 per mil decrease in planktic foraminiferal $\delta^{18}O$ values (Fig. 7D). It is also noticeable in North Atlantic deep water $\delta^{18}O$ values (a ~0.5 per mil decreases at Site 980 and U1308, Fig. 7B and C, respectively) and to a minor degree in the global stack (~0.2 per mil, Fig. 7A). As similar sea surface warming event occurs during the glacial maximum of MIS 10 (at 340 Ka) when the planktic foraminiferal $\delta^{18}O$ values decrease by ~1 per mil (Fig. 7D). In this case, the $\delta^{18}O$ minimum does not have an equivalent feature in any of the benthic records, and it must entirely reflect sea surface hydrographic changes. Thus both glacial maxima are characterized by large instabilities at the sea surface. Then, there is a cold reversal evident as a minor disruption of Termination IV (at 337 Ka) in the global stack, but apparent in large $\delta^{18}O$ swings in benthic foraminiferal $\delta^{18}O$ records from North Atlantic Site 980 and the subtropical Atlantic Sites 1056 and 1063 (Fig. 7A, B, and E, F, respectively). This feature is not apparent in the *G. ruber* $\delta^{18}O$ record, which decreases smoothly during Termination IV (Fig. 7D). Such relatively rapid climatic warming events during glacial intervals and terminations have been observed in other paleoclimate proxy records from regions farther north and east in the Atlantic Ocean (e.g., Stein et al., 2009; Voelker et al., 2010) suggesting that they are of basin-wide significance.

Interglacial MIS 9 differs from the other interglacial intervals MIS 11 and 13 in that, with the exception of the three cold snaps, $\delta^{18}O$ values smoothly follow the long-term trends (Fig. 7C). As noted by Billups et al. (2006) who compare *G. sacculifer* and *G. ruber* data, it is *G. sacculifer* that records lesser fluctuations during MIS 13–15 than *G. ruber*. Therefore the muted variations recorded by *G. ruber* during MIS 9 are not a species artifact. It appears that MIS 9 is different from other interglacials in that it is relatively stable aside from three well defined cold excursions, and thus more akin to interglacial conditions in the North Atlantic (e.g., McManus et al., 1999).

The long-term perspective highlights that during intervals of peak warmth (MIS 13, MIS 11, MIS 9, and MIS 8.5), the two North Atlantic $\delta^{13}C$ records (Sites 980 and U1308) overlap (Fig. 8). It is during these times that millennial-scale $\delta^{13}C$ maxima in the subtropical Site 1063 $\delta^{13}C$ values approach the northern source $\delta^{13}C$ signatures (Fig. 8A). Glacial intervals MIS 12 and 10, on the other hand, are associated with decreasing $\delta^{13}C$ values in the deep North Atlantic (Site U1308) with respect to shallower Site 980 and with lower $\delta^{13}C$ amplitude variations in the deep subtropical Atlantic (Site 1063).

Wavelet analysis summarizes temporal changes in significant millennial-scale variations in the surface (Site 1056/1058 planktic splice) and deep water proxies (Site 1063 benthic splice) (Fig. 9). Significant variations in both records cluster into two bands, a shorter one containing periodicities between ~4 and 8 kyr and a longer one containing periodicities between 8 and 16 kyr. In the planktic foraminiferal $\delta^{18}O$ record, highest spectral power is apparent during the MIS 13/12 transition, most of MIS 12, the MIS 12/11 transition, the MIS 10 maximum, the MIS 10/9 transition, and during the cold snaps of MIS 9 (310–320 Ka) (Fig. 9A). Lower, yet significant, spectral power also occurs during two distinct intervals within MIS 11 (385–390 Ka and 400–410 Ka). In the benthic foraminiferal $\delta^{13}C$ record significant millennial-scale variations occur during the MIS 13/12 transition, all of MIS 11, the MIS 10/9 transition, MIS 9, the MIS 9/8 transition and MIS 8 (Fig. 9B). The glacial maxima of MIS 10 and 12 are characterized by a pronounced lack of any significant millennial-scale variations in the deep water record.

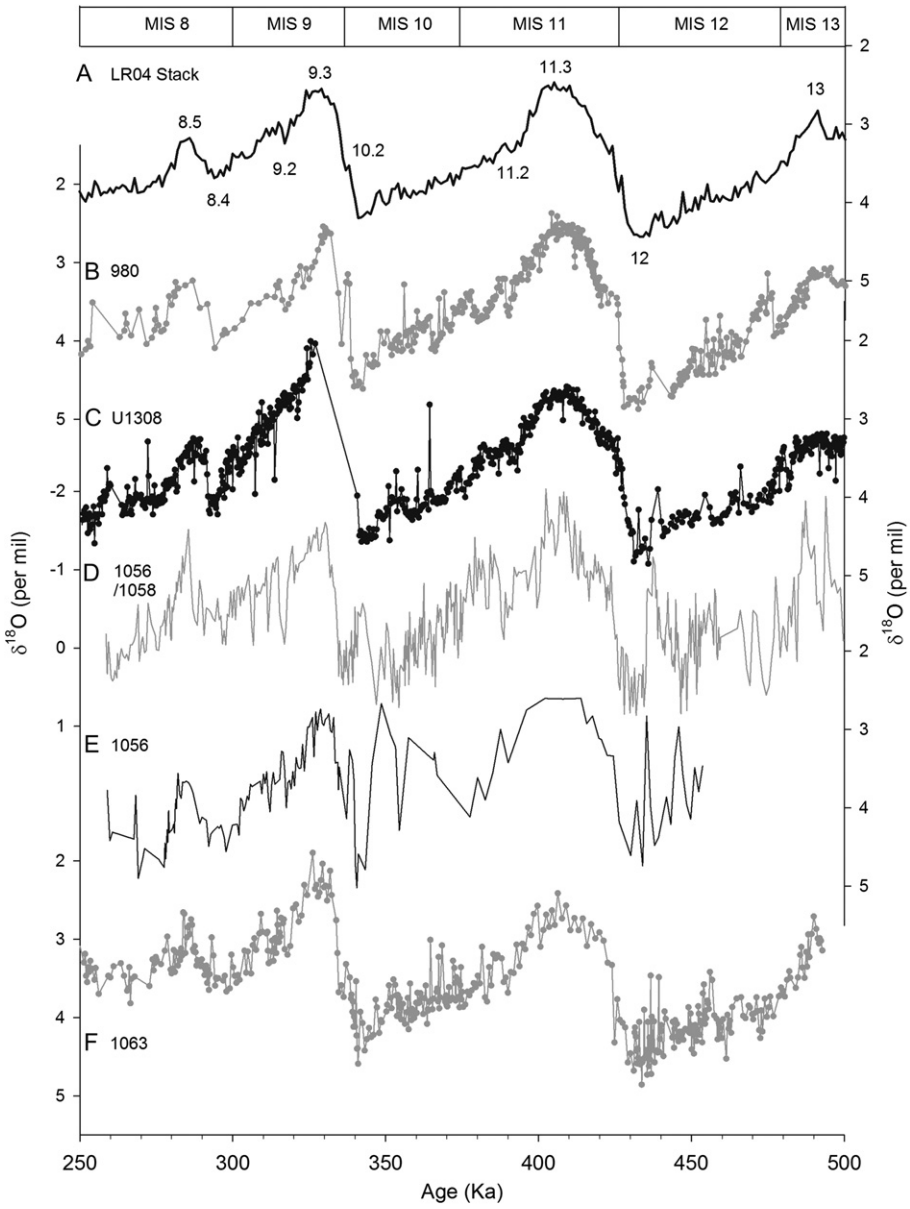

Fig. 7. Correlation of all sites (B, benthic foraminifera from Site 980; C, U1308, D, planktonic foraminifera from Site 1056 and 1058; E, Site 1056 benthic foraminifera; F Site 1063 benthic foraminifera) to the global $\delta^{18}O$ stack of Lisiecki and Raymo (2005) (LR04) (A). The records are correlated using the $\delta^{18}O$ maxima and minima associated with the individual Marine Isotope Stages 8.5 through 13 (labeled). Note that only the MIS 12–13 portion of the planktic foraminiferal record is used for age model purposes. Table 1 provides the data source for each record.

There are only few instances when millennial-scale variations in the planktic $\delta^{18}O$ and benthic $\delta^{13}C$ records occur at the same time. There is only one interval of time when both records display millennial-scale variations in the 8–16 kyr band (during the MIS 10/9 transition) and there are three intervals when both records display millennial-scale variations, but in different bands (MIS 13/12 transition, MIS 11, and MIS 9). These observations imply that there is no consistent co-occurrence in millennial-scale variations between surface and deep water records during the study interval (MIS 8–13).

6. Discussion

In sum, in the northwestern subtropical Atlantic a consistent relationship between deep and surface water hydrographic changes is evident on orbital time scales. Benthic foraminiferal $\delta^{13}C$ values are high during interglacial intervals, and during relatively warm stages as in the case of MIS 8.5. During the terminations (IV and V) as well as the rapid $\delta^{18}O$ decrease within MIS 8 (at ~294 Ka), benthic foraminiferal $\delta^{13}C$ increases are rather synchronous with surface water $\delta^{18}O$ decreases. On the millennial-scale, results show that both the subtropical Atlantic sea surface as well as the deep water regime (at 4600 m water depth) is sensitive to significant suborbital-scale variations. Wavelet analysis demonstrates that millennial-scale variations in planktic foraminiferal $\delta^{18}O$ variations tend to be more prevalent during the glacial intervals while such variations dominate benthic foraminiferal $\delta^{13}C$ values during the interglacial, or less extreme glacial stages (in the case of MIS 8.5).

Enhanced millennial-scale spectral power in the planktic foraminiferal $\delta^{18}O$ record during glacial with respect to interglacial intervals is consistent with the idea of a glacial threshold that once crossed introduces higher frequency variations into North Atlantic

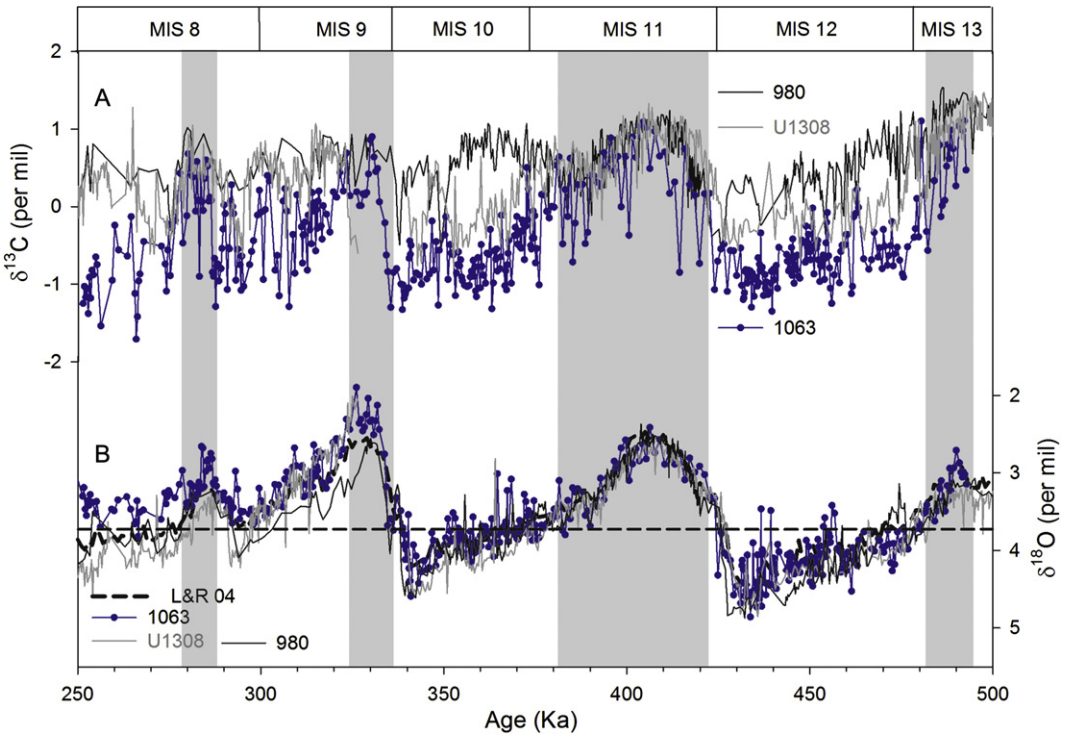

Fig. 8. (A) Comparison of the benthic foraminiferal $\delta^{13}C$ record from Site 1063 (blue circles) to $\delta^{13}C$ values in the North Atlantic source water region (Site 980 black line, Site U1308 grey line). For reference, panel B shows the benthic foraminiferal $\delta^{18}O$ records from Sites 980 (black line, U1308, grey line), Site 1063 (blue circles) and the global stack (heavy dashed line). Vertical grey bars highlight intervals of time when Site 1063 $\delta^{13}C$ values approach those recorded at North Atlantic Sites 980 and U1308. The horizontal dashed line in B corresponds to a value of 3.7 per mil in the global $\delta^{18}O$ stack. Table 1 provides the data source for each record. (For interpretation of the references to colour in this figure legend, the reader is referred to the web version of this article.)

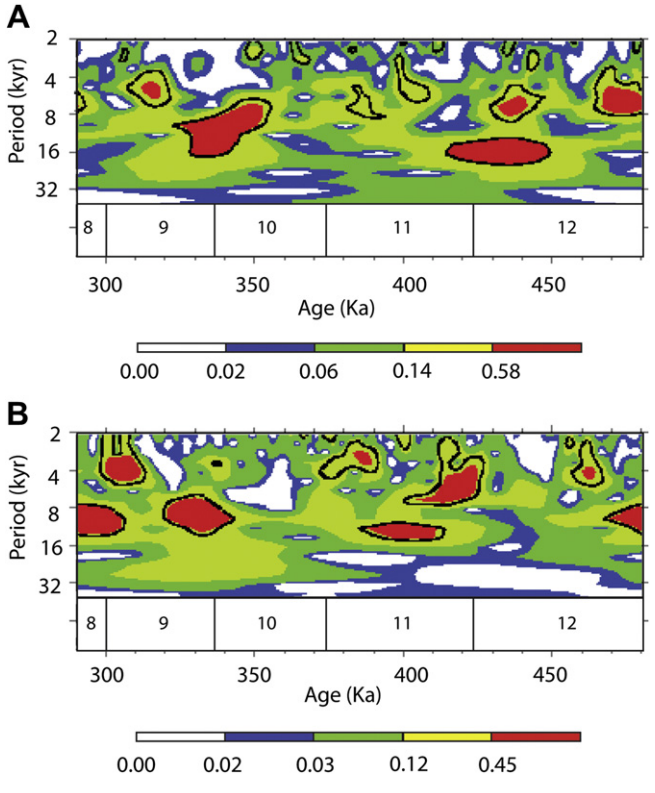

Fig. 9. Wavelet analysis (software provided by *Torrence and Compo*, and available at URL: http://paos.colorado.edu/research/wavelets/) of the Site 1056/1058 planktic $\delta^{18}O$ splice (A) and the Site 1063 *Cibicidoides* $\delta^{13}C$ composite (B). The records were high pass filtered to remove the orbital, glacial to interglacial cycle. Marine Isotope Stages (MIS) are labeled for reference.

surface water proxy records (McManus et al., 1999). This does not mean that the interglacial intervals are stable, as evidenced by the cold snaps during MIS 11 (Billups et al., 2004) and MIS 9 (this study). But it suggests an amplification mechanism operating during glacial intervals with far field effects on the subtropical sea surface. Weirauch et al. (2008) demonstrate that millennial-scale variations in planktic foraminiferal $\delta^{18}O$ values become more prevalent in this region at around 900 Ka coincident with the mid Pleistocene transition toward more extreme Northern Hemisphere glaciations in support of an ice sheet size related mechanism.

The observation that Site 1063 benthic foraminiferal $\delta^{13}C$ variations are high during interglacial and lesser extreme glacial intervals, while notably absent during the glacial maxima of MIS 10 and 12, is also consistent with a concept of threshold crossing. Because intervals of high $\delta^{13}C$ values also correspond to intervals of significant millennial-scale variability, we propose that at 4600 m water depth in the subtropical Atlantic the effects of millennial-scale changes in meridional overturning are felt only while there is a relatively high flux of NADW to this site. Specifically, we observe that the Site 1063 $\delta^{13}C$ variations are high (and North Atlantic $\delta^{13}C$ values overlap) while benthic foraminiferal $\delta^{18}O$ values, as recorded in the global stack, remain below ~3.7 per mil (Fig. 8B). When $\delta^{18}O$ values fall above this threshold such as during glacial stages MIS 10 and 12 there is no evidence for millennial-scale changes in the relative flux of northern-sourced deep waters in the deep subtropical Atlantic Ocean. At these times, AABW must have remained a significant water mass at this water depth as indicated by the decrease in Site U1308 benthic foraminiferal $\delta^{13}C$ values with respect to those at mid-depth Site 980. These geochemical inferences are supported by reconstructions of current flow in the deep western boundary current at BBOR Site 1061 suggesting that the northern-sourced current shoaled during glacial MIS 10 and 12 in

response to enhanced flux of southern sourced waters (Hall and Becker, 2007). In fact, the threshold for such changes reported here (3.7 per mil) is very close to the threshold of 3.8 per mil marking enhanced millennial-scale variations in the sortable silt-derived flow regime of the deep western boundary current at Site 1061 (Hall and Becker (2007).

Because millennial-scale variations in thermohaline circulation are large during interglacial and warm intervals they cannot be driven primarily by processes related to ice sheet size. This is not to rule out that millennial-scale variations do not exist during glacial intervals and that during these times factors such as meltwater affect deep water formation in the North Atlantic (Broecker et al., 1990; Oppo et al., 1995; McManus et al., 2004; Benway et al., 2010). The core depth of Site 1063 is just not sensitive to such changes during glacial maxima because the site is then dominated by AABW. Our results are consistent with reconstructions from the North Atlantic where millennial-scale benthic foraminiferal $\delta^{13}C$ fluctuations remain relatively high regardless of glacial versus interglacial conditions or ice volume thresholds (McManus et al., 1999). Because the deep subtropical Atlantic is more sensitive to changes in deep water circulation than the North Atlantic region (Site 980 is relatively shallow and lies close to the northern component source waters), at least during interglacial intervals, our results evidence that millennial-scale variations in thermohaline circulation persist through interglacial intervals.

Poleward heat transport in surface currents is one possible mechanism that may introduce rapid oscillations into proxy records of thermohaline circulation. Suborbital-scale proxy variations often contain periodicities close to the second and fourth harmonics of precession (e.g., ~10 kyr and ~5 kyr, respectively). Berger et al. (2006), for example, show that harmonics of precession arise from the interactions between precession and eccentricity in equatorial regions as they cause insolation maxima during the solstices as well as the equinoxes. Furthermore, the inter-hemispheric out-of-phase occurrence of precession maxima can lead to precession harmonics in northern hemisphere proxy records via cross-equatorial surface water advection of the southern hemisphere temperature maximum (e.g. Short et al., 1991; McIntyre and Molfino, 1996; Rutherford and D'Hondt, 2000). Second and/or fourth harmonics have been observed in numerous surface water records (e.g., Hagelberg et al., 1994; McIntyre and Molfino, 1996; Ortiz et al., 1999; Weirauch et al., 2008). And, recently it has been shown that both surface and deep water records of the North Atlantic vary on these time scales during the mid Pleistocene (MIS 23–20) in support of tropical insolation as an ultimate source of variability in meridional overturn (Ferretti et al., 2010).

Spectral analysis of the benthic $\delta^{13}C$ record indirectly supports a tropical origin of the millennial-scale variations in the deep water masses. Power spectra more precisely pinpoint the periodicities of millennial-scale peaks in the Site 1063 benthic foraminiferal $\delta^{13}C$ record to 10.2 Ka, 6.7 Ka, 5.1 Ka, and 3.9 Ka (Fig. 10). The peaks at 10.2 Ka and 5.1 Ka are close to the second and fourth harmonic of the 20 kyr precession signal significant in the record (Fig. 10). Thus the periodicities of the millennial-scale peaks are close to the expected harmonics of precessional forcing apparent in the record. Because such periodicities are important in equatorial isolation (Short et al., 1991; Berger et al., 2006), their presence in the subtropical Atlantic deep water record is in line with tropical insolation being an important factor in meridional overturning circulation during the later Pleistocene interglacial intervals.

In the planktic foraminiferal records shown here, however, millennial-scale fluctuations tend to be more pronounced during the glacial than the interglacial intervals (e.g., MIS 12 vs. MIS 11). Although there are some times when surface and deep water records contain variations in the same band, this is not consistent throughout the entire study interval. Therefore we cannot establish a relationship between surface to deep water records across the entire study interval that would provide more direct evidence for a link between changes in meridional heat transport at the sea surface and subsequent deep water formation at high latitudes.

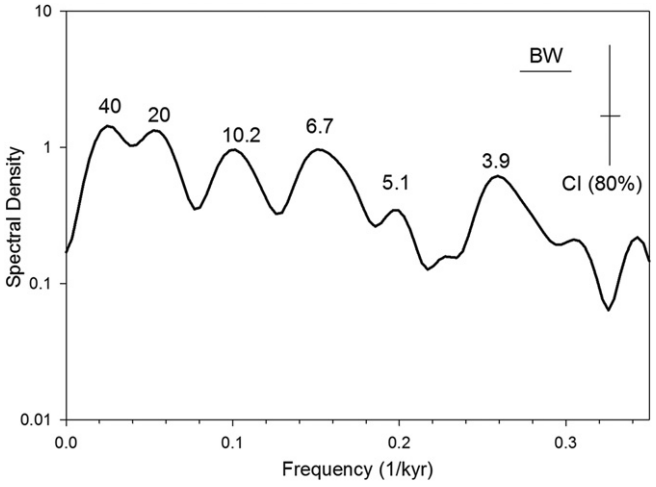

Fig. 10. Spectral analysis of the Site 1063 benthic foraminiferal $\delta^{13}C$ record using Blackman Tuckey methods (Howell et al., 2006). Significant power is concentrated on the orbital periodicities of 40 kyr and 20 kyr, as well as on millennial-scale peaks of 10.2 kyr, 6.7 kyr, 5.1 kyr and 3.9 kyr. The confidence interval (CI) as well as the bandwidth (BW) is given in the figure as vertical and horizontal lines, respectively.

7. Summary and conclusions

We set out to investigate millennial-scale variations in surface and deep water hydrography in the northwestern subtropical Atlantic with an initial focus on MIS 9 and the ultimate goal to compare such variations during two full glacial (MIS 12 and 10) and two full interglacial (MIS 11 and 9) intervals. These records were to test for a link between surface and deep water hydrography as evidence for the association between poleward heat transport and high latitude deep water formation as part of meridional overturning circulation in the Atlantic Ocean. Our results show that there is no simple relationship between planktic and benthic foraminiferal stable isotope records in support of such a link. Instead, we find evidence for significant millennial-scale periodicities, primarily during glacial intervals in the surface water record as recorded by planktic foraminiferal $\delta^{18}O$ values and primarily during interglacial intervals in the deep water record as recorded by benthic foraminiferal $\delta^{13}C$ values. The fact that the millennial-scale variations in the deep water record are pronounced during the warm intervals supports that thermohaline circulation is sensitive to driving forces other than those directly related to ice sheet size. The periodicities in the deep water record are close to the second and fourth harmonic of precessional forcing indirectly supporting the importance of tropical insolation on deep water formation and flow in the North Atlantic.

Acknowledgments

NR and JS thank the NSF for the summer REU at the University of Delaware in which context a portion of the stable isotope records was generated. We also thank Antje Voelker and an anonymous reviewer for valuable suggestions that helped us to improve the manuscript. The study was partially supported by NSF grant OCE-0452666 (KB). This research used samples provided by the

Ocean Drilling Program (ODP). ODP is sponsored by the U.S. National Science Foundation (NSF) and participating countries under the management of the Joint Oceanographic Institutions (JOI), Inc.

References

Bauch, H.A., Erlenkeuser, H., Helmke, J.P., Struck, U., 2000. A paleoclimatic evaluation of marine oxygen isotope stage 11 in the high northern Atlantic (Nordic seas). Global Planet. Change 24, 27–39.

Benway, H.M., McManus, J.F., Oppo, D.W., Cullen, J.L., 2010. Hydrographic changes in the eastern subpolar North Atlantic during the last deglaciation. Quaternary Sci. Rev. 29, 3336–3345.

Berger, A., Loutre, M.F., Mélice, J.L., 2006. Equatorial insolation: from precession harmonics to eccentricity frequencies. Clim. Past Discuss. 2, 519–533.

Bickert, T., Curry, W.B., Wefer, G., 1997. Late Pliocene to Holocene (2.6–0 Ma) western equatorial Atlantic deep-water circulation: Inferences from benthic stable isotopes. doi:10.2973/odp.proc.sr.154.110.1997.

Billups, K., Channell, J., Zachos, J., 2002. Late Oligocene to early Miocene geochronology and paleoceanography from the subantarctic South Atlantic. Paleoceanography 17 (1). doi:10.1029/2000PA000568.

Billups, K., Chaisson, W., Worsnopp, M., Thunell, R., 2004. Millennial-scale fluctuations in subtropical northwestern Atlantic surface ocean thermal stratification. Paleoceanography 19. doi:10.1029/2003PA000990.

Billups, K., Lindley, C., Fisler, J., Martin, P., 2006. Mid Pleistocene climate instability in the subtropical northwestern Atlantic. Global Planet. Change 54, 251–262.

Boyle, E.A., Keigwin, L.D., 1987. North Atlantic thermohaline circulation during the last 20 000 years linked to high latitude surface temperature. Nature 330, 35–40.

Broecker, W., Bond, G., Klas, M., Bonani, G., Wolfli, W., 1990. A salt oscillator in the glacial Atlantic? 1. The concept. Paleoceanography 5 (4), 469–477.

Chaisson, P.W., Poli, M.-S., Thunell, R.C., 2002. Gulf Stream and western boundary undercurrent variations during MIS 10–12 at site 1056, Blake-Bahama outer ridge. Marine Geol. 189, 79–105.

Chapman, M.R., Shackleton, N.J., 1998. Millennial-scale fluctuations in North Atlantic heat flux during the last 150 000 years. EPSL 159, 57–70.

Curry, W., Duplessy, J., Labeyrie, L., Shackleton, N., 1988. Changes in the distribution of $\delta^{13}C$ of deep water ΣCO_2 between the last glaciation and the Holocene. Paleoceanography 3 (3), 317–341.

Desprat, S., Sánchez Goñi, M.F., Duprat, J., Cortijo, E., McManus, J.F., 2008. Millennial-scale climatic variability between 340 000 and 270 000 years ago in SW Europe: evidence from a NW Iberian Margin pollen sequence. Clim. Past Discuss. 4, 375–414.

Deuser, W.G., 1987. Seasonal variations in isotopic composition and deep water fluxes of the tests of perennially abundant planktonic foraminifera of the Sargasso Sea: results from sediment trap collections and their paleoceanographic significance. J. Foraminiferal Res. 17, 14–27.

Dickson, A.J., Beer, C.J., Dempsey, C., Maslin, M.A., Bendle, J.A., McClymont, E.L., Pancost, R.D., 2009. Oceanic forcing of the marine isotope stage 11 interglacial. Nat. Geosci. 2, 428–433. doi:10.1038/ngeo527.

Droxler, A.W., Poore, R., Burckle, L.H. (Eds.), 2003. Earth's Climate and Orbital Eccentricity: The Marine Isotope Stage 11 Question, Geophysical Monograph, 137. American Geophysical Union, Washington, DC.

Erez, J., Luz, B., 1982. Temperature control of oxygen isotope fractionation of cultured planktonic foraminifera. Geochim. Cosmochim. Acta 47, 220–222.

Fairbanks, R.G., Charles, C.D., Wright, J., et al., 1992. Origin of global meltwater pulses. In: Taylor, R.E. (Ed.), Radiocarbon after Four Decades. Springer Verlag, New York, pp. 473–500.

Ferretti, P., Crowhurst, S.J., Hall, M.A., Cacho, I., 2010. North Atlantic millennial-scale climate variability 910 to 790 ka and the role of the equatorial insolation forcing. EPSL 293, 28–41.

Franz, S.O., Tiedemann, R., 2002. Depositional changes along the Blake–Bahama Outer Ridge deep water transect during marine isotope stages 8 to 10 – links to the deep western boundary current. Marine Geol. 189, 107–122.

Grützner, J., Giosan, L., Franz, S.O., Tiedemann, R., Cortijo, E., Chaisson, W.P., Flood, R.D., Hagen, S., Keigwin, L.D., Poli, S., Rio, D., Williams, T., 2002. Astronomical age models for Pleistocene drift sediments from the western north Atlantic (ODP Sites 1056 to 1063). Marine Geol. 189, 5–23.

Hagelberg, T.K., Bond, G., de Menocal, P., 1994. Milankovitch band forcing of sub-Milankovitch climate variability during the Pleistocene. Paleoceanography 9, 545–558. doi:10.1029/94PA00443.

Hagen, S., Keigwin, Lloyd D., 2002. Sea-surface temperature variability and deep water reorganization in the subtropical North Atlantic during isotope stage 2–4. Marine Geol. 189, 145–162.

Hall, I.R., Becker, J., 2007. Deep western boundary current variability in the subtropical northwest atlantic ocean during marine isotope stages 12–10. Geochem. Geophys. Geosyst. 8, Q06013. doi:10.1029/2006GC001518.

Healey, S., Thunell, R., 2004. Millennial-scale variability in western subtropical North Atlantic surface and deepwater circulation during marine isotope stages 11 and 12. Paleoceanography 19. doi:10.1029/2003PA000925.

Helmke, J., Bauch, H., 2003. Comparison of glacial and interglacial conditions between the polar and the subpolar North Atlantic region over the past five climate cycles. Paleoceanography 18.

Hodell, D.A., Charles, C.D., Ninemann, U.S., 2000. Comparison of interglacial stages in the South Atlantic sector of the Southern Ocean for the past 450 kyr: implications for marine isotope stage MIS 11. Glob. Planetary Change 24, 7–26.

Hodell, D.A., Venz, K.A., Charles, C.D., Ninemann, U.S., 2003. Pleistocene vertical carbon isotope gradients in the South Atlantic sector of the Southern Ocean. Geochem. Geophys. Geosystems 3 (1). doi:10.1029/2002GC000367.

Hodell, D.A., Channell, J.E.T., Curtis, J.H., Romero, O.E., Röhl, U., 2008. Onset of "Hudson Strait" Heinrich events in the eastern North Atlantic at the end of the middle Pleistocene transition (~640 ka)? Paleoceanography 23, PA4218. doi:10.1029/2008PA001591.

Howell, P., Posies, N.J., Baughman, B.J., Ochs, L., 2006. ARAND Time Series Analysis Software. Brown University, Providence, RI.

Keigwin, L.G., Jones, G.A., 1994. Western North Atlantic evidence form millennial-scale changes in ocean circulation and climate. J. Geophys. Res. 99, 12,397–12,410.

Keigwin, L.D., Rio, D., Acton, G.D., et al., 1998. Proceedings of the Ocean Drilling Program. Initial Rep. 172, 77–156.

Kroopnick, P.M., 1985. The distribution of $\delta^{13}c$ $o\sigma co_2$ in the world oceans. Deep Sea Res. 32, 57–84.

Löwenmark, L., Hong, W.-L., Yui, T.-F., Hung, G.-W., 2005. A test of different factors influencing the isotopic signal of planktonic foraminifera in surface sediments from the northern South China Sea. Marine Micropaleontology 55, 49–62.

Laskar, J., Joutel, F., Boudin, F., 1993. Orbital, precessional, and insolation quantities for the Earth from -20 Myr to +10 Myr. Astron. Astrophys. 270, 522–533.

Levitus, S., Boyer, T.P., 1994. World Ocean Atlas 1994. In: Temperature, NOAA Atlas NESDIS 4, vol. 4. Nat. Oceanic and Atmos. Admin, Silver Spring, Md, 129 pp.

Levitus, S., Burgett, R., Boyer, T.P., 1994. World Ocean Atlas 1994. In: Salinity, NOAA Atlas NESDIS 34, vol. 3. Nat. Oceanic and Atmos. Admin, Silver Spring, Md, 111 pp.

Lisiecki, L.E., Raymo, M.E., 2005. A Pliocene-Pleistocene stack of 57 globally distributed benthic δ18O records. Paleoceanography 20, PA1003. doi:10.1029/2004PA001071.

Lisiecki, L.E., Raymo, M.E., 2009. Diachronous benthic δ18O responses during late Pleistocene terminations. Paleoceanography 24, PA3210. doi:10.1029/2009PA001732.

MacAyeal, D.R., 1993. Growth/purge oscillations of the Laurentide ice sheet as a cause of the North Atlantic's Heinrich events. Paleoceanography 8, 775–784.

Mackensen, A., Bickert, T., Fischer, G., 1999. Stable carbon isotopes in benthic foraminifera: proxies for deep and bottom water circulation and new production. In: Wefer, G. (Ed.), Use of Proxies in Paleoceaongraphy: Examples from the South Atlantic. Springer-Verlag, Berlin Heidelberg, pp. 229–254.

Matsumoto, K., Lynch-Stieglitz, J., 2003. Persistence of Gulf Stream separation during the last glacial period:Implications for current separation theories. Journal of Geophysical Research 108, C6, doi:10.1029/2001JC000861.

Mayewski, P.A., Meeker, L.D., Twickler, M.S., Whitlow, S.W., Ynag, Q., Lyons, W.B., Prentice, M., 1997. Major features and forcing of high-latitude northern hemisphere atmospheric circulation using a 110 000 yea long glaciochemical series. J. Geophys. Res. 102 (C12), 26,345–26,366.

McIntyre, A., Molfino, B., 1996. Forcing of Atlantic equatorial and subpolar millennial cycles by precession. Science 274, 1867–1870. doi:10.1126/science.274.5294.1867.

McManus, J.F., Oppo, D.W., Cullen, J.L., 1999. A 0.5 million year record of millennial-scale climate variability in the North Atlantic. Science 283, 971–974.

McManus, J.F., Francois, R., Gherardi, J.-M., Keigwin, L.D., Brown-Leger, S., 2004. Collapse and rapid resumption of Atlantic meridional circulation linked to deglacial climate changes. Nature 428, 834.

Oppo, D.W., Lehman, S.J., 1995. Suborbital timescale variability of North Atlantic deep water during the past 200 000 years. Paleoceanography 10, 901–910.

Oppo, D.W., McManus, J.F., Cullen, J.L., 1998. Abrupt climate events 500 000 to 340 000 years ago: evidence from subpolar North Atlantic sediments. Science 279, 1335–1338.

Oppo, D.W., Keigwin, L.D., McManus, J.F., 2001. Persistent suborbital variability in marine isotope stage 5 and termination II. Paleoceanography 16, 280–292.

Ortiz, J., Mix, A., Harris, A., 1999. Diffuse spectral reflectance as a proxy for percent carbonate content in North Atlantic sediments. Paleoceanography 14, 171–186. doi:10.1029/1998PA900021.

Pickard, G.L., Emery, W.J., 1990. Descriptive Physical Oceanography: An Introduction. Pergamon Press, 320 pp.

Poli, M.S., Thunell, R.C., Rio, D., 2000. Millennial-scale changes in North Atlantic deep water circulation during marine isotope stages 11 and 12; Linkage to Antarctic climate. Geology 28, 807–810.

Rühlemann, C., Mulitza, S., Müller, P.J., Wefer, G., Zahn, R., 1999. Warming of the tropical Atlantic Ocean and slowdown of thermohaline circulation during the last deglaciation. Nature 402, 511–514.

Rahmstorf, S., 2002. Ocean circulation and climate during the past 120 000 years. Nature 419, 207–214.

Raymo, M.E., Ruddiman, W.F., Shackleton, N.J., Oppo, D.W., 1990. Evolution of Atlantic-Pacific $\delta^{13}C$ gradients over the last 2.5 m.y. Earth Planetary Sci. Lett. 97, 353–368.

Ruddiman, W., 2007. The early anthropogenic hypothesis: challenges and responses. Rev. Geophys. 45, RG4001. doi:10.1029/2006RG000207.

Rutherford, S., D'Hondt, S., 2000. Early onset and tropical forcing of 100 000-year Pleistocene glacial cycles. Nature 408, 72–75.

Schmidt, M.W., Vautravers, M.J., Spero, H.J., 2006. Rapid subtropical North Atlantic salinity oscillations across Dansgaard/Oeschger cycles. Nature 443, 561–564.

Schmitz, W.J., McCartney, M.S., 1993. On the North Atlantic circulation. Rev. Geophys. 31 (1), 29–49.
Schulz, M., Berger, W.H., Sarnthein, M., Grootes, P.M., 1999. Amplitude variations of 1450-year climate oscillations during the last 100 000 years linked to fluctuations of continental ice. Geophys. Res. Lett. 26, 3385–3388.
Short, D.A., Mengel, J.G., Crowley, T.J., Hyde, W.T., North, G.R., 1991. Filtering of Milankovitch cycles by Earth's geography. Quat. Res. 35, 157–173.
Skinner, L.C., Shackleton, N.J., 2005. An Atlantic lead over Pacific deep-water change across termination I: implications for the application of the marine isotope stage stratigraphy. Quat. Sci. Rev. 24, 571–580.
Stein, R., Hefter, J., Grützner, J., Voelker, A., Naafs, B.D.A., 2009. Variability of surface water characteristics and Heinrich-like events in the Pleistocene midlatitude North Atlantic Ocean: biomarker and XRD records from IODP Site U1313 (MIS 16–9). Paleoceanography 24, PA2203. doi:10.1029/2008PA001639.
Thunell, R.C., Poli, Maria S., Rio, Domenico, 2002. Changes in deep and intermediate water properties in the western North Atlantic during marine isotope stages 11–12: evidence from ODP Leg 172. Marine Geol. 189, 63–77.
Vidal, L., Labeyrie, L., Cortijo, E., Arnold, M., Duplessy, J.C., Michel, E., Becqué, S., van Weering, T.C.E., 1997. Evidence for changes in the North Atlantic deep water linked to meltwater surges during the Heinrich events. EPSL 146, 13–27.
Voelker, A., L. de Abreu. A review of abrupt climate change events in the north-eastern Atlantic ocean(Iberian margin): latitudinal, longitudinal, and vertical gradients, geophysical monograph Series, in press.
Voelker, A.H.L., Rodrigues, T., Stein, R., Hefter, J., Billups, K., Oppo, D., McManus, J., Grimalt, J.O., 2010. Variations in mid-latitude North Atlantic surface water properties during the mid-Brunhes (MIS 9–14) and their implications for the thermohaline circulation. Clim. Past. 6, 531–552.
Wang, L., 2000. Isotopic signals in two morphotypes of *Globigerinoides ruber* (white) from the South China sea: implications for monsoon climate change during the last glacial cycle. Palaeogeography, Palaeoclimatology, Palaeoecology 161, 381–394.
Weirauch, D., Billups, K., Martin, P., 2008. Evolution of millennial-scale climate variability during the mid Pleistocene. Paleoceanography 23, PA3216. doi:10.1029/2007PA001584.